EINDHOVEN UNIVERSITY OF TECHNOLOGY

Deposition temperature dependence of material and Si surface passivaion properties of O3-based atomic layer deposited Al2O3-based films and stacks

Citation for published version (APA):
Bordihn, S., Mertens, V., Müller, J. W., & Kessels, W. M. M. (2014). Deposition temperature dependence of material and Si surface passivaion properties of O3-based atomic layer deposited Al2O3-based films and stacks. *Journal of Vacuum Science and Technology A*, *32*, 01A128-1/7. https://doi.org/10.1116/1.4852855

DOI:
10.1116/1.4852855

Document status and date:
Published: 01/01/2014

Document Version:
Publisher's PDF, also known as Version of Record (includes final page, issue and volume numbers)

Please check the document version of this publication:

• A submitted manuscript is the version of the article upon submission and before peer-review. There can be important differences between the submitted version and the official published version of record. People interested in the research are advised to contact the author for the final version of the publication, or visit the DOI to the publisher's website.
• The final author version and the galley proof are versions of the publication after peer review.
• The final published version features the final layout of the paper including the volume, issue and page numbers.

Link to publication

General rights
Copyright and moral rights for the publications made accessible in the public portal are retained by the authors and/or other copyright owners and it is a condition of accessing publications that users recognise and abide by the legal requirements associated with these rights.

• Users may download and print one copy of any publication from the public portal for the purpose of private study or research.
• You may not further distribute the material or use it for any profit-making activity or commercial gain
• You may freely distribute the URL identifying the publication in the public portal.

If the publication is distributed under the terms of Article 25fa of the Dutch Copyright Act, indicated by the "Taverne" license above, please follow below link for the End User Agreement:

www.tue.nl/taverne

Take down policy
If you believe that this document breaches copyright please contact us at:

openaccess@tue.nl

providing details and we will investigate your claim.

Download date: 17. Nov. 2023

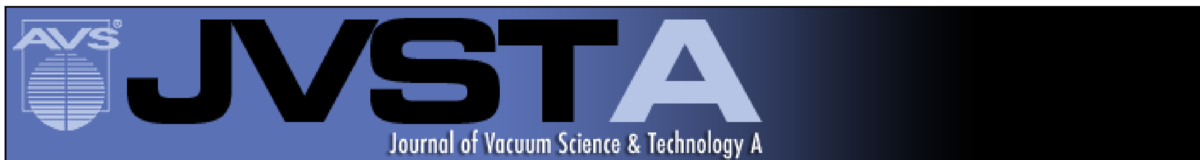

Deposition temperature dependence of material and Si surface passivation properties of O3-based atomic layer deposited Al2O3-based films and stacks

Stefan Bordihn, Verena Mertens, Jörg W. Müller, and W. M. M. (Erwin) Kessels

Citation: Journal of Vacuum Science & Technology A **32**, 01A128 (2014); doi: 10.1116/1.4852855
View online: http://dx.doi.org/10.1116/1.4852855
View Table of Contents: http://scitation.aip.org/content/avs/journal/jvsta/32/1?ver=pdfcov
Published by the AVS: Science & Technology of Materials, Interfaces, and Processing

Re-register for Table of Content Alerts

Create a profile. 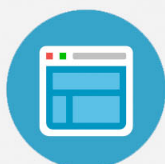 Sign up today!

Redistribution subject to AVS license or copyright; see http://scitation.aip.org/termsconditions. Download to IP: 131.155.151.148 On: Tue, 07 Jan 2014 13:03:11

Deposition temperature dependence of material and Si surface passivation properties of O_3-based atomic layer deposited Al_2O_3-based films and stacks

Stefan Bordihn[a)]
Department of Applied Physics, Eindhoven University of Technology, P.O. Box 513, 5600 MB Eindhoven, The Netherlands and Hanwha Q CELLS GmbH, Sonnenallee 17-21, 06766 Bitterfeld-Wolfen, Germany

Verena Mertens and Jörg W. Müller
Hanwha Q CELLS GmbH, Sonnenallee 17-21, 06766 Bitterfeld-Wolfen, Germany

W. M. M. (Erwin) Kessels[b)]
Department of Applied Physics, Eindhoven University of Technology, P.O. Box 513, 5600 MB Eindhoven, The Netherlands

(Received 22 October 2013; accepted 6 December 2013; published 26 December 2013)

The material composition and the Si surface passivation of aluminum oxide (Al_2O_3) films prepared by atomic layer deposition using $Al(CH_3)_3$ and O_3 as precursors were investigated for deposition temperatures (T_{Dep}) between 200 °C and 500 °C. The growth per cycle decreased with increasing deposition temperature due to a lower Al deposition rate. In contrast the material composition was hardly affected except for the hydrogen concentration, which decreased from [H] = 3 at. % at 200 °C to [H] < 0.5 at. % at 400 °C and 500 °C. The surface passivation performance was investigated after annealing at 300 °C–450 °C and also after firing steps in the typical temperature range of 800 °C–925 °C. A similar high level of the surface passivation performance, i.e., surface recombination velocity values <10 cm/s, was obtained after annealing and firing. Investigations of Al_2O_3/SiN_x stacks complemented the work and revealed similar levels of surface passivation as single-layer Al_2O_3 films, both for the chemical and field-effect passivation. The fixed charge density in the Al_2O_3/SiN_x stacks, reflecting the field-effect passivation, was reduced by one order of magnitude from $3\cdot10^{12}\,cm^{-2}$ to $3\cdot10^{11}\,cm^{-2}$ when T_{Dep} was increased from 300 °C to 500 °C. The level of the chemical passivation changed as well, but the total level of the surface passivation was hardly affected by the value of T_{Dep}. When firing films prepared at of low T_{Dep}, blistering of the films occurred and this strongly reduced the surface passivation. These results presented in this work demonstrate that a high level of surface passivation can be achieved for Al_2O_3-based films and stacks over a wide range of conditions when the combination of deposition temperature and annealing or firing temperature is carefully chosen. © *2014 American Vacuum Society*.
[http://dx.doi.org/10.1116/1.4852855]

I. INTRODUCTION

Aluminum oxide (Al_2O_3) thin films prepared by atomic layer deposition (ALD) or plasma enhanced chemical vapor deposition (PECVD) have been identified as a high quality surface passivation material for *p*-type surfaces of Si solar cells.[1] The excellent passivation performance can be attributed to a high level of chemical and field-effect passivation. The latter is generated by a high negative fixed charge density in the Al_2O_3 films.[2–4] An important process parameter for the preparation of high quality Al_2O_3 films is the deposition temperature as previously established for films grown in ALD processes with an O_2-plasma as oxidant,[5,6] with H_2O (Ref. 7) and for films grown by PECVD processes.[8,9] So far, no systematic study has appeared that addresses the relation between material properties and surface passivation performance of Al_2O_3 films grown in ALD processes with O_3 as oxidant. O_3 can be beneficial over alternative oxidants such as H_2O due to its higher reactivity. Furthermore, it is more straightforward to implement an O_3-based ALD process in high throughput batch reactors than ALD processes based on O_2 plasma. Apparently, the availability of high throughput deposition equipment is an essential requirement for the implementation of ALD Al_2O_3 processes in manufacturing lines of Si solar cells.

In this work, the Si surface passivation performance and material properties of Al_2O_3 films deposited by $Al(CH_3)_3$ and O_3 as precursor and oxidant were studied while addressing the influence of the deposition temperature in particular. These studies are relevant as the surface chemistry and the substrate oxidation by the O_3-based process is quite different from ALD processes based on H_2O or O_2 plasma as oxidants.[10–13] This might have implications for the surface passivation performance of the Al_2O_3 films as well as its temperature dependence. First, the composition and material properties of the Al_2O_3 films were compared with those prepared by ALD processes using H_2O and an O_2-plasma as oxidants. Second, the surface passivation performance of the Al_2O_3 films was investigated after annealing and firing. In particular, the influence on the field-effect passivation was addressed by analyzing the films by corona charging

[a)]Electronic mail: s.bordihn2@q-cells.com
[b)]Electronic mail: w.m.m.kessels@tue.nl

Redistribution subject to AVS license or copyright; see http://scitation.aip.org/termsconditions. Download to IP: 131.155.151.148 On: Tue, 07 Jan 2014 13:03:11

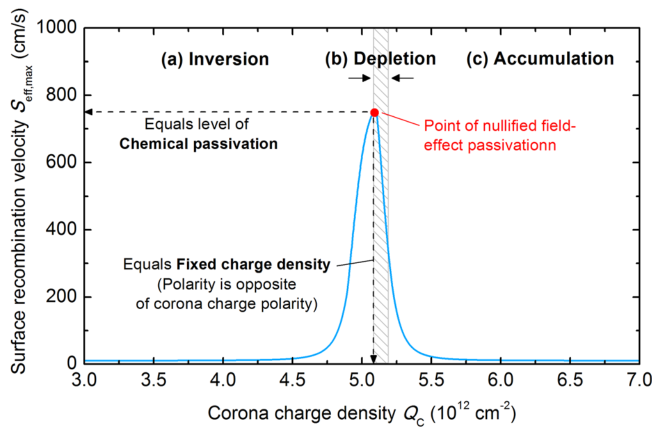

FIG. 1. (Color online) Schematic illustration of effective surface recombination velocity $S_{eff,max}$ as a function of deposited corona charge density Q_C for a passivation material with negative fixed charge incorporated. Indicated are the corresponding energy band conditions, i.e., inversion, depletion, and accumulation.

experiments. The study is complemented by results on Al_2O_3/SiN_x stacks, which are considered because previous studies reported a higher level of surface passivation after firing when using Al_2O_3/SiN_x stacks instead of single-layer Al_2O_3 films.[14] From the systematic studies, the relation between the material properties and the surface passivation performance of Al_2O_3 films is discussed.

II. EXPERIMENT

A. Sample preparation

Czochralski (Cz) grown *n*-type Si wafers (12.5 × 12.5 cm^2) were used as substrates with a thickness of 180 μm and a resistivity of 2–4 Ω·cm. The wafers were cleaned in a KOH based wet chemical solution to remove the saw damage before carrying out a standard Radio Cooperation of America cleaning procedure. The Al_2O_3 films were deposited simultaneously on both sides of the wafers during 330 ALD-cycles by using $Al(CH_3)_3$ and O_3 as precursor and oxidant, respectively. The dosing and purge times were 1 s–3 s–3 s–6 s for $Al(CH_3)_3$–purge–O_3–purge, respectively. The cycle time was 13 s in total. The deposition temperature (T_{Dep}) was varied between 200 °C and 500 °C. The T_{Dep} refers to the set temperature of the reactor walls of the hot wall reactor. A 30 min time interval has been employed between loading the wafers in the reactor and the start of the ALD process to allow for equilibration of wafer temperature. On half of the wafer set, SiN_x films were deposited at 350 °C in a PECVD process using a linear microwave plasma source. The SiN_x films were also deposited on both wafer sides to create a symmetric sample structure.

The surface passivation performance of single-layer Al_2O_3 films and Al_2O_3/SiN_x stacks was determined after annealing and after firing. For the single-layer Al_2O_3 films annealing was carried out at temperatures (T_{Anneal}) between 300 °C and 450 °C for 10 min in N_2 ambient. The surface passivation was analyzed only for $T_{Anneal} > T_{Dep}$. The firing step was carried out at a peak temperature (T_{Firing}) between 850 °C and 925 °C for several seconds. The Al_2O_3/SiN_x stacks were either annealed at 400 °C or fired at 850 °C, i.e., no investigations at other temperatures were carried out. The firing step was used to mimic the thermal budget of the metal contact formation process of industrial-type Si solar cells.

B. Material analysis

The film thickness was determined by spectroscopic ellipsometry for films deposited on float zone (Fz) Si wafers (12.5 × 12.5 cm^2) with shiny etched surfaces. These samples were prepared similarly as the films deposited on the Cz Si wafers. The atomic composition of the films was analyzed by the combination of Rutherford backscattering spectroscopy (RBS) and elastic recoil detection. From the film thickness, the growth per cycle (GPC) and the film thickness nonuniformity $(d_{max} - d_{min})/(2 \cdot d_{average})$[15] were calculated using 137 measurement points equally distributed over the wafer area of 149.3 cm^2. The number of Al atoms deposited per cycle was calculated from the RBS data and the number of deposition cycles carried out.

C. Surface passivation analysis

The effective minority carrier lifetime τ_{eff} was measured as a function of the excess carrier density Δn by using the photoconductance decay technique in the transient and generalized mode.[16] The surface passivation was expressed in terms of an upper limit of the effective surface recombination velocity $S_{eff,max}$, which was calculated from the value of τ_{eff} at $\Delta n = 10^{14}$ cm^{-3} using the expression: $S_{eff,max} = W/2 \cdot (\tau_{eff}^{-1} - \tau_{Auger}^{-1})$ with W the wafer thickness and correcting for the Auger lifetime τ_{Auger} by employing the parameterization proposed by Richter *et al.*[17]

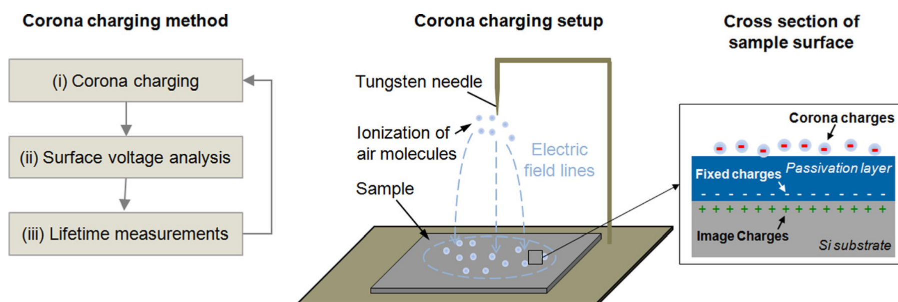

FIG. 2. (Color online) Illustration of the corona charging experiment: (i) corona charging, (ii) surface voltage analysis, and (iii) lifetime measurements are carried out sequentially and repeated time over time. The corona charging setup and and a cross sectional view of the sample are also shown.

Redistribution subject to AVS license or copyright; see http://scitation.aip.org/termsconditions. Download to IP: 131.155.151.148 On: Tue, 07 Jan 2014 13:03:11

D. Corona charging experiments

The level of field-effect passivation and chemical passivation was investigated by corona charging experiments. In these experiments, a procedure was repeated that consists of corona charge deposition, surface voltage measurements, and surface passivation measurements.[18,19] Corona charges were deposited on top of the passivated wafer surface. The corona charges are ionizing air molecules that are created at a tungsten needle by a high electric field caused by a voltage of ~6 kV applied to the needle. To investigate the fixed charge density Q_f present in a passivation film corona charges with the opposite polarity of Q_f need to be deposited. By Kelvin probe measurements, the surface voltage can be obtained and used to calculate the corona charge density Q_C on top of the wafer surface with the help of the following expression: $Q_C = V_{surf} \cdot \varepsilon_0 \cdot \varepsilon_r / (d \cdot e)$, with V_{surf} the surface voltage, e the elementary charge, d the layer thickness, ε_r the relative permittivity of the film, and ε_0 the vacuum permittivity. The relative permittivity is substituted by an average value when stacks of dielectric materials are investigated.[20] As a result of the corona charging experiments, a $S_{eff,max}(Q_C)$-plot is obtained, which has commonly a bell-like curved shape. The field-effect passivation was determined from the position of the peak value of the $S_{eff,max}(Q_C)$-plot as at this point the deposited Q_C compensates Q_f. Therefore, at this point, only the chemical passivation contributes to the total level of surface passivation. Consequently, the peak value of $S_{eff,max}$ can be regarded as a measure for the level of the chemical passivation. The $S_{eff,max}(Q_C)$-plot and the corona charging setup are illustrated schematically in Figs. 1 and 2, respectively.

III. RESULTS AND DISCUSSION

A. Material properties of Al_2O_3 films

Properties such as GPC, film thickness, and thickness nonuniformity reveal information about the ALD process. The properties obtained for the Al_2O_3 films in this work are listed in Table I. In Fig. 3, the data are compared to results reported previously by Potts *et al.* for films grown in ALD processes that used H_2O and O_2-plasma as oxidant.[5] For the O_3-process, the GPC values decreased from 0.9 Å to 0.6 Å with increasing T_{Dep}, and therefore, the GPC values were in the same range as the H_2O and O_2-plasma data. The data show that the density of deposited Al atoms per cycle decreased with increasing T_{Dep} while the mass density stayed almost constant at ~2.9 g/cm^3. Consequently, the reduction in Al atoms deposited per unit area in every cycle is the reason for the lower film thickness and lower GPC when

TABLE I. Properties of atomic layer deposited Al_2O_3 films deposited at various temperatures (set value of the heater). The number of ALD cycles was 330. The film thickness was measured by spectroscopic ellipsometry and the atomic composition by RBS/ERD measurements. The film thickness nonuniformity was calculated on basis of 137 measurement points equally distributed over the wafer area of 149.3 cm^2.

	Deposition temperature			
	200 °C	300 °C	400 °C	500 °C
Film thickness (nm)	30 ± 0.2	28 ± 0.3	26 ± 0.4	21 ± 0.1
Thickness nonuniformity (%)	—[a]	±5	±2	±3
Growth per cycle (Å/cycle)	0.9 ± 0.2	0.8 ± 0.1	0.8 ± 0.1	0.6 ± 0.1
Al (10^{14} at. cm^{-2} cycle^{-1})	2.8 ± 0.5	2.8 ± 0.5	2.6 ± 0.5	2.1 ± 0.5
[O]/[Al]	1.7 ± 0.1	1.7 ± 0.1	1.5 ± 0.1	1.6 ± 0.1
[H] (at. %)	3.0 ± 0.1	2.3 ± 0.1	<0.1	<0.4
Al_2O_3 mass density (g/cm^3)	2.7 ± 0.2	3.0 ± 0.2	2.8 ± 0.2	2.9 ± 0.2

[a]Not measured.

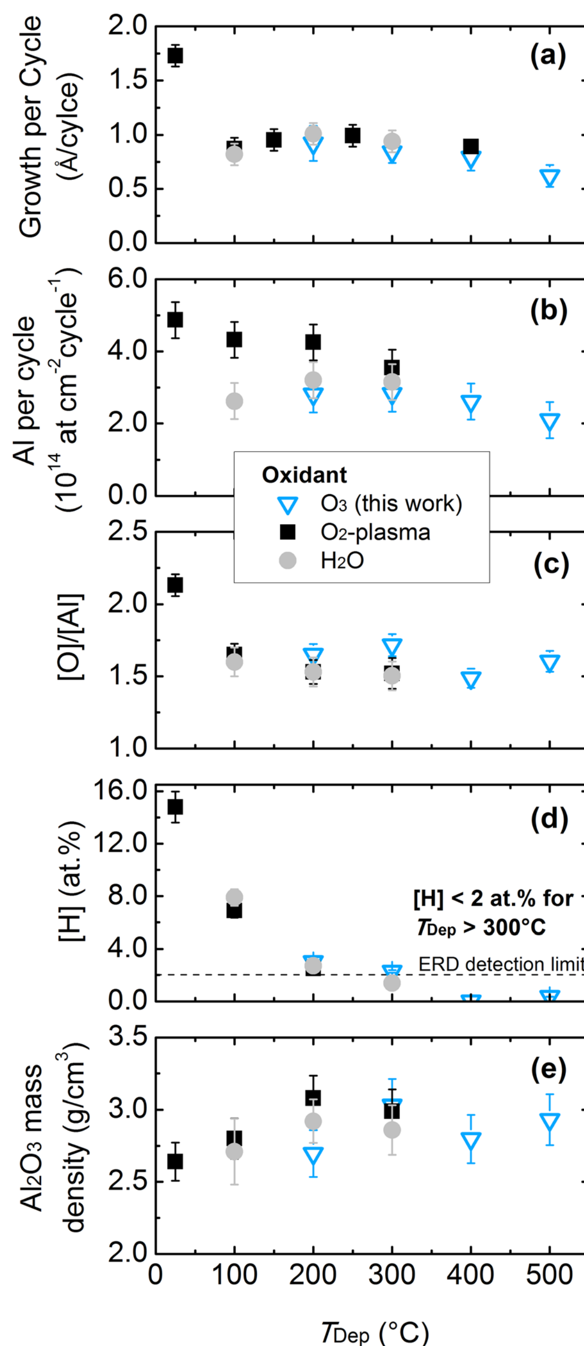

FIG. 3. (Color online) Film properties for Al_2O_3 films deposited by the O_3-based process at various deposition temperatures: (a) growth per cycle; (b) deposited Al atoms per cycle; (c) [Al]/[O] ratio; (d) hydrogen content [H]; and (e) Al_2O_3 mass density. Data were obtained from ellipsometry and RBS/ERD measurements. For comparison purposes, data of Al_2O_3 films deposited by ALD with H_2O and O_2-plasma are given as reported by Potts *et al.* in Ref. 5.

Redistribution subject to AVS license or copyright; see http://scitation.aip.org/termsconditions. Download to IP: 131.155.151.148 On: Tue, 07 Jan 2014 13:03:11

TABLE II. Upper limit of the effective surface recombination velocities $S_{eff,max}$ (cm/s) of single-layer Al_2O_3 films prepared at various deposition temperatures (set value of the hot wall reactor temperature) after annealing in N_2 for 10 min and after firing for several seconds. The uncertainty in the data represents the standard deviation extracted from five measurements over each sample.

		Deposition temperature			
	Temperature	200 °C	300 °C	400 °C	500 °C
Annealing	300 °C	26 ± 9			
	350 °C	12 ± 5	34 ± 11		
	400 °C	7 ± 2	14 ± 6		
	450 °C	5 ± 2	6 ± 2	124 ± 70	
Firing	800 °C	12 ± 5	8 ± 3	66 ± 47	64 ± 30
	850 °C	26 ± 7	9 ± 1	9 ± 2	20 ± 16
	910 °C	13 ± 2	6 ± 2	6 ± 1	6 ± 1
	925 °C	9 ± 1	5 ± 1	4 ± 1	5 ± 1

going to higher T_{Dep}. The hydrogen concentration decreased from [H] = 3 at. % at T_{Dep} = 200 °C to [H] < 0.5 at. % at T_{Dep} = 400 °C and 500 °C. Overall, the trend of the deposited Al atoms per cycle [O]/[Al] ratio and [H] content was found to be quite similar to the data reported for Al_2O_3 films prepared with H_2O and an O_2-plasma as oxidants.

B. Surface passivation of single-layer Al_2O_3 films

The influence of the deposition temperature on the surface passivation performance, which is expressed in terms of an upper limit of the effective surface recombination velocity $S_{eff,max}$, is shown in Table II. The data are given after annealing and after firing at various temperatures. With increasing annealing temperature, the $S_{eff,max}$-values of films grown at T_{Dep} = 200 °C decreased from 26 cm/s to 5 cm/s. The same trend was observed for films prepared at T_{Dep} = 300 °C with $S_{eff,max}$ decreasing from 34 cm/s to 6 cm/s when T_{Anneal} increased from 350 °C to 450 °C. The corresponding $\tau_{eff}(\Delta n)$-values showed an upward shift with annealing temperature over the entire measured injection range, see Fig. 4(a). To reveal more insight into the passivation mechanism behind this shift, corona charging experiments were carried out. The obtained $S_{eff,max}(Q_C)$-plots are shown in Fig. 4(b). The Q_f-value, represented by Q_C when $S_{eff,max}$ has its maximum, increased only slightly when increasing T_{Anneal} from 350 °C to 450 °C. However, the peak value of $S_{eff,max}$ was reduced significantly, from 1430 cm/s to 230 cm/s, with increasing T_{Anneal}. Consequently, the improvement of the surface passivation with increasing annealing temperature can be attributed to an improved chemical passivation. Depositing the Al_2O_3 films at 400 °C and annealing this films at 450 °C did not result in low $S_{eff,max}$.

After firing, the surface recombination velocities of Al_2O_3 films grown at T_{Dep} = 300 °C were <10 cm/s independently of the used T_{Firing}. In contrast Al_2O_3 films deposited at T_{Dep} = 400 °C and 500 °C yielded a factor of ten lower $S_{eff,max}$-values when T_{Firing} increased from 800 °C to 925 °C. Remarkable was that all Al_2O_3 films, i.e., deposited between 200 °C and 500 °C, resulted in $S_{eff,max}$-values <10 cm/s after firing at the highest temperature, i.e., T_{Firing} = 925 °C. After firing, the highest surface passivation level is achieved for the single-layer Al_2O_3 films prepared at T_{Dep} between 300 °C and 500 °C (see Table II). Apparently, same $S_{eff,max}$-values, within the experimental error, can be achieved after firing and after annealing when using optimized process conditions.

TABLE III. Surface recombination velocities $S_{eff,max}$ (cm/s) of Al_2O_3/SiN_x stacks with the Al_2O_3 films prepared at various deposition temperatures and annealed for 10 min in N_2 or fired for a couple of seconds in ambient conditions.

		Deposition temperature			
	Temperature	200 °C	300 °C	400 °C	500 °C
Annealing	400 °C	11 ± 6	14 ± 6		
Firing	850 °C	30 ± 4	8 ± 2	9 ± 2	19 ± 10

C. Surface passivation of Al_2O_3/SiN_x stacks

The surface passivation study of single-layer Al_2O_3 films was complemented by investigations of the surface passivation served by Al_2O_3/SiN_x stacks. The obtained $S_{eff,max}$-values of the stacks after annealing and after firing are given in Table III. After annealing, the $S_{eff,max}$-values of the

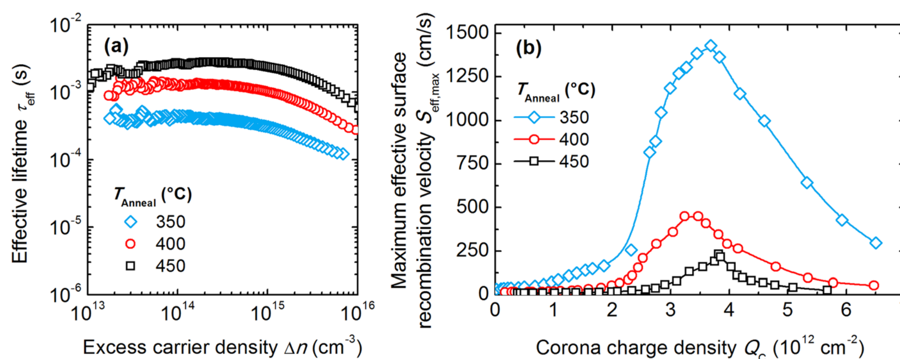

FIG. 4. (Color online) (a) Injection dependent minority carrier lifetime $\tau_{eff}(\Delta n)$ obtained by photoconductance decay measurements in the transient mode for Al_2O_3 films prepared at 300 °C and annealed for 10 min in N_2 at temperatures ranging from 350 to 450 °C. (b) $S_{eff,max}(Q_C)$-plots obtained by corona charging experiments for the same films as in (a). Lines serve as a guide to the eye.

Redistribution subject to AVS license or copyright; see http://scitation.aip.org/termsconditions. Download to IP: 131.155.151.148 On: Tue, 07 Jan 2014 13:03:11

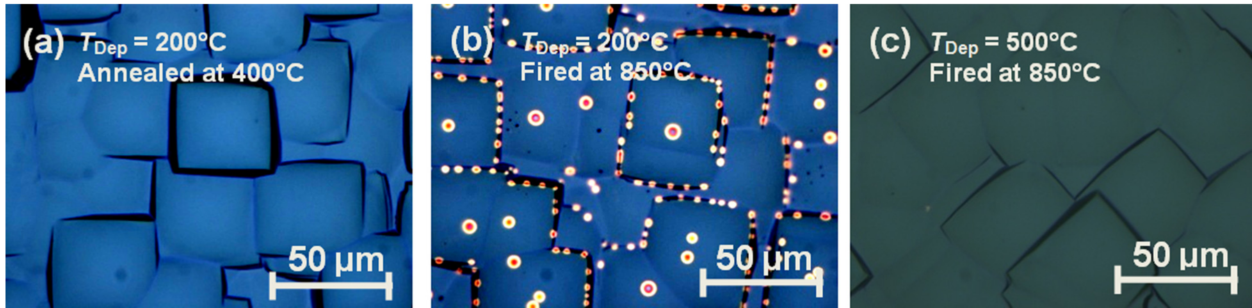

FIG. 5. (Color online) Optical microscopy images of Cz sample surfaces coated with Al_2O_3/SiN_x stacks. Al_2O_3/SiN_x stacks with (a) Al_2O_3 film deposited at 200 °C after anneal at 400 °C, (b) Al_2O_3 film deposited at 200 °C after firing at 850 °C, and (c) Al_2O_3 film deposited at 500 °C after firing at 850 °C.

stacks were found to be similar to the one achieved for single-layer Al_2O_3 films within the experimental error, see Tables II and III, respectively. After firing at 850 °C, the $S_{eff,max}$-values of the stacks decreased from 30 cm/s to 9 cm/s when T_{Dep} of the Al_2O_3 films increased from 200 °C to 400 °C. A similar behavior was observed for the single-layer Al_2O_3 films for that particular firing temperature. Stacks with Al_2O_3 films deposited at 500 °C yielded a $S_{eff,max}$-value of 19 cm/s. The higher $S_{eff,max}$-values obtained for stacks after firing with the Al_2O_3 films deposited at 200 °C could possibly be (partly) related to the effect of blistering. Blistering is a local delamination of the Al_2O_3 films, and consequently, it can cause a reduction of the surface passivation performance.[21–24] Optical microscopy images of the Al_2O_3/SiN_x stacks are shown in Fig. 5 after annealing [Fig. 5(a)] and after firing [Fig. 5(b)] and are also compared to images of a stack after firing with the Al_2O_3 films deposited at 500 °C [Fig. 5(c)]. The stacks with the Al_2O_3 films deposited at 200 °C showed blistering only after firing and not after annealing, see Figs. 5(a) and 5(b), respectively. The higher temperature and the faster temperature ramp rate play therefore a role for blistering. Furthermore, blistering seems to be related to the higher hydrogen content of the Al_2O_3 films deposited at 200 °C. The hydrogen concentration was [H] = 3 at. % for films deposited at 200 °C but [H] < 0.5 at. % for films deposited at 500 °C. These observations are in line with results reported by Hennen *et al.* who correlated the hydrogen content of the films and the formation of blisters.[25]

Corona charging experiments were carried out to investigate the mechanism responsible for the trend of the $S_{eff,max}$-values with changing deposition temperature. The surface passivation performance is shown in Fig. 6(a) in terms of the $\tau_{eff}(\Delta n)$ for the Al_2O_3/SiN_x stacks after firing at 850 °C. The values of τ_{eff} increased over a wide range of Δn-values when higher deposition temperatures were used for the Al_2O_3 films. The discrepancy between the results shown in Table III and in Fig. 6(a) for the stacks with Al_2O_3 films grown at 200 °C and 500 °C can be attributed to the fact that for the corona charging experiments one sample point ($4 \times 4\,cm^2$ in area) is considered whereas the $S_{eff,max}$-values given in Table III are an average value obtained from five measurement points distributed over the sample area. The $S_{eff,max}(Q_C)$-plots are shown in Fig. 6(b) (no corona charging experiments could be carried out for the sample suffering from blistering, i.e., for $T_{Dep} = 200\,°C$). Increasing T_{Dep} yielded lower Q_C-values for which the maximum in $S_{eff,max}$ was reached, from $Q_C = 3 \cdot 10^{12}\,cm^{-2}$ at $T_{Dep} = 300\,°C$ to $3 \cdot 10^{11}\,cm^{-2}$ at $T_{Dep} = 500\,°C$. Hence, the negative fixed charge density, as a measure for the field-effect passivation, decreased by one order of magnitude when going to higher deposition temperatures. For the chemical passivation, no clear trend could be discerned but the stack with the Al_2O_3 films deposited at $T_{Dep} = 300\,°C$ showed the highest level of chemical passivation. Remarkable was that the stacks with Al_2O_3 films grown at 300 °C and 400 °C showed a clear difference in the peak

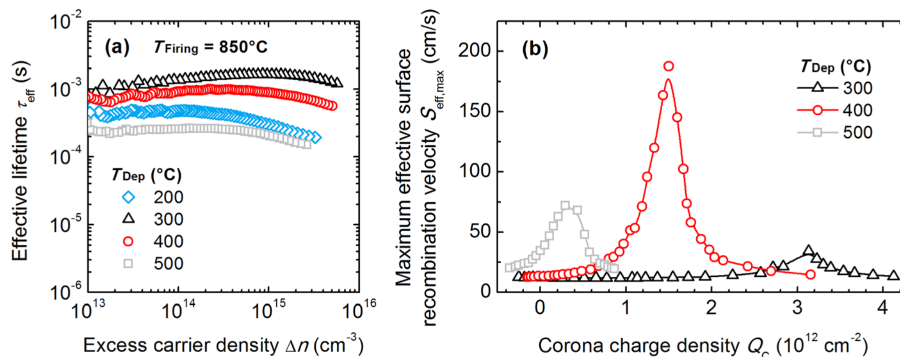

FIG. 6. (Color online) (a) Injection dependent minority carrier lifetime $\tau_{eff}(\Delta n)$ for Al_2O_3/SiN_x stacks after firing at 850 °C. The deposition temperature for the Al_2O_3 films is indicated. (b) $S_{eff,max}(Q_C)$-plots obtained by corona charging for the Al_2O_3/SiN_x stacks after firing at 850 °C. No data is available for the Al_2O_3 films grown at 200 °C. Lines serve as a guide to the eye.

Redistribution subject to AVS license or copyright; see http://scitation.aip.org/termsconditions. Download to IP: 131.155.151.148 On: Tue, 07 Jan 2014 13:03:11

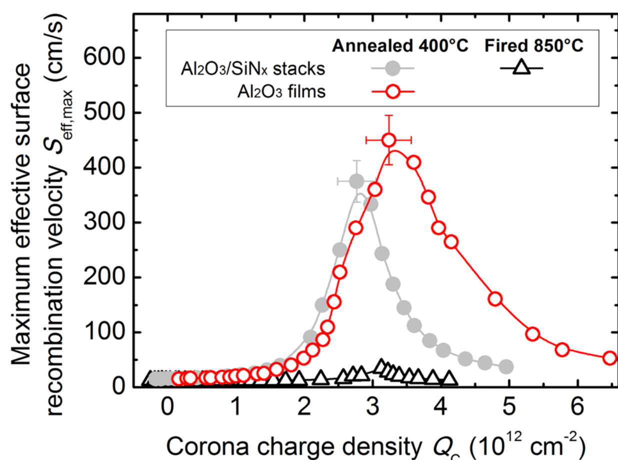

FIG. 7. (Color online) $S_{eff,max}(Q_C)$-plots obtained by corona charging experiments for single-layer Al_2O_3 films and Al_2O_3/SiN_x stacks with Al_2O_3 films grown at 300 °C. The data for the single-layer film are shown after annealing at 400 °C and for the stacks after annealing at 400 °C and after firing at 850 °C. Lines serve as a guide to the eye.

value of $S_{eff,max}$ (the peak values differ by ∼150 cm/s) and also a clear difference in Q_f (Q_f differs by $\sim 1.5 \cdot 10^{12}$ cm^{-2}). Yet, their $S_{eff,max}$-values (without corona charges) are very similar as shown in Table III. This holds also for the τ_{eff}-value at $\Delta n = 10^{14}$ cm^{-3} as shown in Fig. 6(a).

The corona charging experiments were also used to investigate whether the SiN_x capping layer deposition affected the field-effect and chemical passivation of the underlying Al_2O_3 films. These experiments were triggered by the fact that the SiN_x films can have a fixed charge density with the opposite charge polarity compared to the Al_2O_3 films,[24] which could potentially compensate (partially) the fixed charge density in the Al_2O_3 films. In Fig. 7, the $S_{eff,max}(Q_C)$-plot of single-layer Al_2O_3 films after annealing is compared to those of Al_2O_3/SiN_x stacks after annealing and after firing. After annealing, the peak value of $S_{eff,max}$ of the stacks resulted in slightly lower values while the peak was also narrower than for the single-layer Al_2O_3 films. This indicates a slightly better chemical passivation for the stacks that can possibly be related to the deposition of the SiN_x capping layer that leads to an additional thermal budget, i.e., an additional anneal. The narrower peak can be related to a change in the capture cross section ratio of electron and holes.[26] The $S_{eff,max}(Q_C)$-plot of the stacks after firing demonstrates the improvement of the chemical passivation due to the firing process when SiN_x layers are present. The peak value of $S_{eff,max}$ is strongly reduced due to a passivation of surface defects by hydrogen. This hydrogen is released from the Al_2O_3 and/or SiN_x films during the firing process.[27] Moreover, the SiN_x film can act as a kind of diffusion barrier for the hydrogen in the Al_2O_3 films increasing the flux of hydrogen toward the Si interface. The field-effect passivation of the Al_2O_3 films was not affected by the SiN_x capping process nor the firing process, which is in line with recently published results for Al_2O_3/SiN_x stacks with a different combination of layer thicknesses.[28]

IV. CONCLUSIONS

The material properties and surface passivation performance of Al_2O_3 films deposited by ALD with O_3 as oxidant were studied for films prepared at various deposition temperatures. The Al_2O_3 films of the O_3-based ALD process showed similar material properties as Al_2O_3 films deposited by ALD using an O_2 plasma or H_2O. It was found that the surface passivation performance of the films obtained after annealing at moderate temperatures (around 400 °C) resulted in a similar high level of the surface passivation performance as obtained after firing at high temperatures (around 900 °C). The high level of surface passivation is demonstrated by low effective surface recombination velocities <10 cm/s. Analysis of the surface passivation mechanisms of the Al_2O_3-based films and stacks revealed that the field-effect passivation depends on the deposition temperature whereas the chemical passivation is mainly affected by the annealing temperature. When combining low deposition temperatures and firing steps, the blistering can occur, which can result in a reduction of the surface passivation performance. Finally, it can be concluded that a multitude of temperature conditions can induce a high level of surface passivation as long as the combination of deposition temperature and annealing or firing temperature is carefully chosen.

ACKNOWLEDGMENTS

This work was supported by the German Ministry for Environment, Nature Conservation and Nuclear Safety (BMU) under Contract No. 0325150 ("ALADIN"). The authors thank W. M. Arnoldbik (AccTec) for the RBS/ERD measurements and W. Keuning (TU/e) for assisting with the spectroscopic ellipsometry. I. Förster, J. Reinhold, and A. Eifler are acknowledged for the assistance with the Al_2O_3 and SiN_x depositions.

[1]J. Schmidt, A. Merkle, R. Brendel, B. Hoex, M. C. M. van de Sanden, and W. M. M. Kessels, Prog. Photovolt. **16**, 461 (2008).
[2]G. Agostinelli, A. Delabie, P. Vitanov, Z. Alexieva, H. F. W. Dekkers, S. De Wolf, and G. Beaucarne, Sol. Energy Mater. Sol. Cells **90**, 3438 (2006).
[3]B. Hoex, S. B. S. Heil, E. Langereis, M. C. M. van de Sanden, and W. M. M. Kessels, Appl. Phys. Lett. **89**, 042112 (2006).
[4]B. Hoex, J. Schmidt, P. Pohl, M. C. M. van de Sanden, and W. M. M. Kessels, J. Appl. Phys. **104**, 044903 (2008).
[5]S. E. Potts, W. Keuning, E. Langereis, G. Dingemans, M. C. M. van de Sanden, and W. M. M. Kessels, J. Electrochem. Soc. **157**, P66 (2010).
[6]S. E. Potts, G. Dingemans, C. Lachaud, and W. M. M. Kessels, J. Vac. Sci. Technol. A **30**, 021505 (2012).
[7]B. Liao, R. Stangl, F. Ma, Z. Hameiri, T. Müller, D. Chi, A. G. Aberle, C. S. Bhatia, and B. Hoex, J. Appl. Phys. **114**, 094505 (2013).
[8]G. Dingemans, M. C. M. van de Sanden, and W. M. M. Kessels, Electrochem. Solid State **13**, H76 (2010).
[9]P. Saint-Cast, D. Kania, M. Hofmann, J. Benick, J. Rentsch, and R. Preu, Appl. Phys. Lett. **95**, 151502 (2009).
[10]D. N. Goldstein, J. A. McCormick, and S. M. George, J. Phys. Chem. C **112**, 19530 (2008).
[11]E. Langereis, J. Keijmel, M. C. M. van de Sanden, and W. M. M. Kessels, Appl. Phys. Lett. **92**, 231904 (2008).
[12]J. Kwon, M. Dai, M. D. Halls, and Y. J. Chabal, Appl. Phys. Lett. **97**, 162903 (2010).
[13]V. R. Rai, V. Vandalon, and S. Agarwal, Langmuir **26**, 13732 (2010).
[14]G. Dingemans, P. Engelhart, R. Seguin, F. Einsele, B. Hoex, M. C. M. van de Sanden, and W. M. M. Kessels, J. Appl. Phys. **106**, 114907 (2009).

Redistribution subject to AVS license or copyright; see http://scitation.aip.org/termsconditions. Download to IP: 131.155.151.148 On: Tue, 07 Jan 2014 13:03:11

[15]A. G. Aberle, Prog. Photovolt. **8**, 473 (2000).
[16]R. A. Sinton and A. Cuevas, Appl. Phys. Lett. **69**, 2510 (1996).
[17]A. Richter, S. W. Glunz, F. Werner, J. Schmidt, and A. Cuevas, Phys. Rev. B **86**, 165202 (2012).
[18]S. W. Glunz, D. Biro, S. Rein, and W. Warta, J. Appl. Phys. **86**, 683 (1999).
[19]S. Dauwe, "Low-temperature surface passivation of crystalline silicon and its application to the rear side of solar cells," Ph.D. dissertation, Dept. Phys., Univ. of Hanover, Hanover, Germany, 2004.
[20]S. Chatterjee, S. K. Samanta, H. D. Banerjee, and C. K. Maiti, Semicond. Sci. Technol. **17**, 993 (2002).
[21]T. Lüder, T. Lauermann, A. Zuschlag, G. Hahn, and B. Terheiden, Energy Procedia **27,** 426 (2012).
[22]B. Vermang, H. Goverde, A. Uruena A. Lorenz, E. Cornagliotti, A. Rothschild, J. John, J. Poortmans, and R. Mertens, Sol. Energy Mater. Sol. Cells **101,** 204 (2012).
[23]P. Saint-Cast, D. Kania, R. Heller, S. Kühnhold, M. Hofmann, J. Rentsch, and R. Preu, Appl. Surf. Sci. **258**, 8371 (2012).
[24]G. Dingemans and W. M. M. Kessels, J. Vac. Sci. Technol. A **30**, 040802 (2012).
[25]L. Hennen, E. H. A. Granneman, and W. M. M. Kessels, *Proceedings of the 38th IEEE Photovoltaic Specialists Conference*, Austin, TX, 3–8 June 2012, 001049–001054.
[26]A. G. Aberle, *Crystalline Silicon Solar Cells: Advanced Surface Passivation and Analysis*, (University of New South Wales, Sydney, Australia, 1999).
[27]H. F. W. Dekkers, "Study and optimization of dry process technologies for thin crystalline silicon solar cell manufacturing," Ph.D. dissertation, Dept. Ing., Katholieke Univ. of Leuven, Leuven, Belgium, 2008.
[28]S. Bordihn, J. A. van Delft, M. M. Mandoc, J. W. Müller, and W. M. M. Kessels, IEEE J. Photovolt. **3**, 970 (2013).

Redistribution subject to AVS license or copyright; see http://scitation.aip.org/termsconditions. Download to IP: 131.155.151.148 On: Tue, 07 Jan 2014 13:03:11